NeuroImage 257 (2022) 119308

Contents lists available at ScienceDirect

NeuroImage

journal homepage: www.elsevier.com/locate/neuroimage

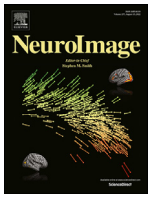

Cortical beta burst dynamics are altered in Parkinson's disease but normalized by deep brain stimulation

K. Amande M. Pauls[a,b,*], Olesia Korsun[b,c], Jukka Nenonen[d], Jussi Nurminen[b], Mia Liljeström[b,c], Jan Kujala[c,e], Eero Pekkonen[a,b], Hanna Renvall[a,b,c]

[a] Department of Neurology, Helsinki University Hospital and Department of Clinical Neurosciences (Neurology), University of Helsinki, Helsinki, Finland
[b] BioMag Laboratory, HUS Medical Imaging Center, University of Helsinki, Aalto University, and Helsinki University Hospital, Helsinki, Finland
[c] Department of Neuroscience and Biomedical Engineering, Aalto University School of Science, Aalto University, Helsinki, Finland
[d] Megin Oy, Espoo, Finland
[e] Department of Psychology, University of Jyväskylä, Jyväskylä, Finland

ARTICLE INFO

Keywords:
Parkinson's disease
Magnetoencephalography
Beta burst
Deep brain stimulation
Oscillatory activity
Resting state

ABSTRACT

Exaggerated subthalamic beta oscillatory activity and increased beta range cortico-subthalamic synchrony have crystallized as the electrophysiological hallmarks of Parkinson's disease. Beta oscillatory activity is not tonic but occurs in 'bursts' of transient amplitude increases. In Parkinson's disease, the characteristics of these bursts are altered especially in the basal ganglia. However, beta oscillatory dynamics at the cortical level and how they compare with healthy brain activity is less well studied. We used magnetoencephalography (MEG) to study sensorimotor cortical beta bursting and its modulation by subthalamic deep brain stimulation in Parkinson's disease patients and age-matched healthy controls. We show that the changes in beta bursting amplitude and duration typical of Parkinson's disease can also be observed in the sensorimotor cortex, and that they are modulated by chronic subthalamic deep brain stimulation, which, in turn, is reflected in improved motor function at the behavioural level. In addition to the changes in individual beta bursts, their timing relative to each other was altered in patients compared to controls: bursts were more clustered in untreated Parkinson's disease, occurring in 'bursts of bursts', and re-burst probability was higher for longer compared to shorter bursts. During active deep brain stimulation, the beta bursting in patients resembled healthy controls' data. In summary, both individual bursts' characteristics and burst patterning are affected in Parkinson's disease, and subthalamic deep brain stimulation normalizes some of these changes to resemble healthy controls' beta bursting activity, suggesting a non-invasive biomarker for patient and treatment follow-up.

1. Introduction

Parkinson's disease (PD) is a common neurodegenerative condition which causes loss of dopaminergic neurons in the substantia nigra, giving rise to the cardinal symptoms of PD. Exaggerated subthalamic beta (13–30 Hz) oscillatory activity (Brown et al., 2001; Levy et al., 2002) and increased beta range cortico-subthalamic synchrony (Hirschmann et al., 2011; Litvak et al., 2011; Marsden et al., 2001; Oswal et al., 2016; Sharott et al., 2018) have crystallized as the electrophysiological hallmarks of these structural changes. The amplitude of subthalamic beta activity correlates with measures of motor disability (Neumann et al., 2016), and both administration of levodopa (Kühn et al., 2006; Levy et al., 2002; Priori et al., 2004; Ray et al., 2008) and deep brain stimulation (DBS) (Kühn et al., 2008; Oswal et al., 2016; Ray et al., 2008) reduce subthalamic beta oscillatory activity. Furthermore, the extent of both DBS and levodopa-induced beta modulation are proportionate to patients' motor performance (Kühn et al., 2008, 2006; Oswal et al., 2016).

Beta oscillatory activity is not tonic but occurs in 'bursts' of transiently increased amplitude (Feingold et al., 2015; Sherman et al., 2016). In primates, the bursting is modulated in a task-dependent and brain-area dependent manner (Feingold et al., 2015). The burst pattern appears to be altered in PD and is modulated by therapy: Both levodopa (Tinkhauser et al., 2017b) and adaptive DBS (Tinkhauser et al., 2017a) shift burst duration towards shorter bursts, and this shift is linked to clinical improvements in motor symptoms (Tinkhauser et al., 2017b, 2017a). Effects of conventional DBS on beta bursting in the subthalamic nucleus (STN) are more varied: stimulation intensity dependent reduction in beta power and mean burst duration has been described (Kehnemouyi et al., 2021), whereas in other studies it only affected burst

* Corresponding author at: BioMag Laboratory, HUS Medical imaging Center, Helsinki University Hospital, Haartmaninkatu, 00290 Helsinki, Finnland.
E-mail address: amande.pauls@hus.fi (K. Amande M. Pauls).

https://doi.org/10.1016/j.neuroimage.2022.119308.
Received 9 December 2021; Received in revised form 12 April 2022; Accepted 10 May 2022
Available online 13 May 2022.

amplitude (Tinkhauser et al., 2017a) but did not modify bursting duration nor rate (Schmidt et al., 2020). Exaggerated beta activity can be observed in other nodes of the oscillatory loop, e.g., the internal part of the globus pallidus (GPi) (Eisinger et al., 2020; Piña-Fuentes et al., 2019), where its amplitude correlates positively with clinical impairment (Eisinger et al., 2020). Synchrony within basal ganglia structures, and between basal ganglia and motor cortex, has been shown to increase during beta bursts both in animal studies (Cagnan et al., 2019; Yu et al., 2021) and in PD patients (Cagnan et al., 2019; Tinkhauser et al., 2018, 2017b), and the increased synchrony is reduced by levodopa (Tinkhauser et al., 2017b).

Cortical sensorimotor spontaneous beta bursting in PD has been studied less extensively and only rarely compared with controls. Earlier findings suggest that the cortex entrains STN beta activity: Cortical beta oscillations lead subthalamic activity (Oswal et al., 2016; Sharott et al., 2018), and subthalamic neurons are sensitive to the magnitude of fluctuations in cortical beta oscillations and show a beta-frequency specific resonance (Baaske et al., 2020). PD patients have longer cortical beta bursts than essential tremor patients (O'Keeffe et al., 2020), and reduced burst rates after levodopa withdrawal compared to healthy controls, while burst amplitude and duration remain unchanged (Vinding et al., 2020). In nonhuman primates, parkinsonism is associated with an increased incidence of beta bursts with longer duration and higher amplitude in the low beta band (8–20 Hz) in both the STN and GPi, but not in the primary motor cortex (Yu et al., 2021).

Most studies investigating beta bursting in PD and its modulation by DBS have been carried out intra- or postoperatively in subcortical structures, but so far little is known about the effects of chronic therapeutic DBS on cortical beta burst dynamics in PD. Importantly, studying cortical burst dynamics allows a direct comparison between healthy individuals and PD patients. In the present study, we used magnetoencephalography (MEG) to study cortical beta bursting in PD patients with DBS_{OFF} and DBS_{ON} and in age-matched healthy controls. We tested the hypothesis that beta bursting changes demonstrated subcortically can be observed in the sensorimotor cortex and that they are modulated by chronic DBS, which, in turn, is reflected in improved motor function. Beta bursting with DBS_{ON} should thus resemble healthy controls' data. Finally, we investigated the hypothesis that it is not only individual bursts, but their timing relative to each other that is altered in PD compared to controls.

2. Materials and methods

2.1. Subjects

We recruited 16 patients with advanced Parkinson's disease (PD, akinetic-rigid $n = 6$, mixed $n = 10$) who had been on chronic subthalamic DBS therapy (cDBS) for a minimum of 5 months (mean 7.6 months, range 5–14 months). All patients had stable stimulation settings and oral pharmacotherapy. The DBS stimulation was based on either an Activa PC system (Medtronic Inc.), or a St. Jude Medical Infinity™ system (Abbott); with both devices the stimulation parameters were considered standard. Patients' epidemiological and clinical data are given in Table 1. 21 controls matched for age, gender and handedness were recruited from different studies. All studies were approved by Helsinki University Hospital or Aalto University Ethical Committees, and all participants gave their written informed consent to participate. Group-level information can be found in Table 2.

2.2. Data collection & experimental paradigm

Patient measurements were carried out after overnight withdrawal of medication ($n = 13$), or while patients were taking their normal medication ($n = 3$), with (a) cDBS ON and (b) cDBS OFF. During the measurements, patients were sitting under the neuromagnetometer relaxed and with their eyes open for a minimum of 5 min per DBS condition.

Table 1
Patient information.

Pat. no.	sex	age	disease duration (years)	time since surgery (months)	PD subtype	UPDRS ON	UPDRS OFF	LED (mg)	DBS left (contacts/amplitude/ frequency/duration)	DBS right (contacts/amplitude/ frequency/duration)
1	f	70	20	6	mixed	25	36	652	11A, 1.2 mA, 130 Hz, 60 µs	3A, 1.0 mA, 130 Hz, 60 µs
2	f	57	13	13	akinetic-rigid	12	25	320	11C, 2.8 mA, 130 Hz, 60 µs	2A, 1.6 mA, 130 Hz, 60 µs
3	m	60	14	8	mixed	11	38	642.5	10A, 2.6 mA, 160 Hz, 60 µs	2A, 2.3 mA, 160 Hz, 60 µs
4	f	74	8	7	mixed	21	39	380	10ABC, 3.7 mA, 130 Hz, 60 µs	2ABC, 3.0 mA, 130 Hz, 60 µs
5	f	61	12	9	akinetic-rigid	20	35	1183	10A, 1.4 mA, 200 Hz, 60 µs	2A, 1.4 mA, 130 Hz, 60 µs
6	f	65	17	14	akinetic-rigid	12	22	180	11A, 2.2 mA, 130 Hz, 60 µs	2C, 1.6 mA, 130 Hz, 60 µs
7	m	44	10	10	mixed	16	43	1060	10C, 2.1 mA, 170 Hz, 60 µs	3C, 2.4 mA, 170 Hz, 110 µs
8	m	60	11	7	mixed	20	39	752.5	11B, 2.1 mA, 150 Hz, 80 µs	3C, 2.0 mA, 150 Hz, 80 µs
9	m	66	13	6	mixed	16	31	908.5	11C, 2.3 mA, 160 Hz, 60 µs	3C, 1.8 mA, 160 Hz, 60 µs
10	f	58	16	6	akinetic-rigid	34	50	500	11ABC, 1.6 mA, 130 Hz, 60 µs	2C, 2.0 mA, 130 Hz, 60 µs
11	m	68	18	5	akinetic-rigid	12	28	880.5	11ABC, 0.6 mA, 130 Hz, 60 µs	2A, 1.1 mA, 160 Hz, 60 µs
12	f	56	11	6	mixed	6	24	1378	11A, 1.9 mA, 130 Hz, 40 µs	3AC, 1.7 mA, 130 Hz, 60 µs
13	m	54	11	7	mixed	14	51	420	11A, 1.9 mA, 90 Hz, 60 µs	3A, 2.1 mA, 130 Hz, 60 µs
14	m	47	8	6	mixed	6	45	580	9-, 2.5 V, 180 Hz, 60 µs	1-, 2.3 V, 180 Hz, 60 µs
15	m	36	9	5	mixed	26	71	210	9-, 3.0 V, 130 Hz, 60 µs	2-, 3 V, 130 Hz, 60 µs
16	m	68	10	7	akinetic-rigid	23	33	427	10-, 2.6 V, 150 Hz, 120 µs	1-, 2.9 V, 150 Hz, 60 µs
Mean +/- std	7 f, 9 m	59 +/- 10.1	12.6 +/- 3.6	7.6 +/- 2.7	mixed n=10, akinetic-rigid n=6	17.1 +/- 7.6	38.1 +/- 12.3	654.6 +/- 350.1	143.8 +/- 26 Hz, 63.8 +/−16.7 µs	143.8 +/−17.5 Hz, 64.4 +/−13.1 µs

Table 2
Group-level information.

	Patients (n=16)	Controls (n=21)	
Age (years) +/- std	59.0 +/- 10.1	60.6 +/- 9.5	p=0.59 §
Sex	7f, 9m	10 f, 11 m	p=0.37 §§
Handedness	right n=12, left n=1, n.a. n=3	right n=20, ambidextrous n=1	p=0.85 §§
beta frequency (Hz) peak +/- std	19.8 +/- 2.2	19.6 +/- 2.7	p=0.73§
left	20.0 +/- 2.3	19.4 +/- 2.7	p=0.51§
right	19.7 +/- 2.1	19.8 +/- 2.7	p=0.85§

§ Two-sided independent samples T-test.
§§ Chi-squared test.

Three patients measured ON medication used controlled release medications (n = 2, patient 14: selegiline 10 mg x 1, levodopa/carbidopa CR 200/50 mg 1/2 × 4, rotigotine 6 mg x 1; patient 15: pramipexole CR 2.1 mg x 1) or had a dosage interval >6 h (n = 1, patient 16: levodopa/carbidopa/entacapone 50 mg x 3, levodopa/carbidopa CR 1/2 × 1, pramipexole CR 1,02 mg x 1, levodopa/benserazide dispersible 100 mg x1). After each measurement, patients' motor symptoms were assessed using the UPDRS III motor score, and a UPDRS III hemibody score was obtained (sum of UPDRS III items 20–26 for left and right extremities separately).

MEG recordings were performed with a 306-channel whole-head MEG system (Elekta Neuromag® and TRIUX^{TM}, both from Megin Oy, Helsinki, Finland) in a magnetically shielded room (ETS-Lindgren, Eura, Finland). Four or five head localization coils were applied in continuous head position indicator (cHPI) tracking of the head position inside the MEG helmet (Uutela et al., 2001). Control data were collected with a sampling frequency of 600 Hz (n = 6) without continuous head position indicator measurement (cHPI), or 1 kHz (n = 15) with cHPI. Patient data were collected with a sampling frequency of 1–3 kHz (1 kHz n = 3, 2 kHz n = 12, 3 kHz n = 1) with cHPI. Head position estimation and movement compensation were performed offline from the cHPI signals (Taulu and Kajola, 2005). Due to interference between the DBS stimulation and cHPI frequencies, cHPI occasionally failed. During later measurements, we increased HPI coil frequencies to prevent interference with common DBS stimulation frequencies.

2.3. Preprocessing

MEG data were preprocessed using spatiotemporal signal space separation (tSSS, (Taulu and Simola, 2006)) implemented in MaxFilter software (Megin Oy, Helsinki, Finland). We used an experimental version of MaxFilter (version 3.0, not commercially available) which contains some extensions to avoid difficulties encountered with the commercial version 2.2 (see the supplementary material for the details). After head position estimations, the data were lowpass filtered at 100 Hz, followed by tSSS suppression of artefact waveforms caused by DBS stimulation, using a correlation limit of 0.8 for efficient tSSS removal of artefacts (Medvedovsky et al., 2009). cHPI was available in 12 out of 16 patients and was used to compensate for head movements. To further compensate for the effect of different patient head positions on sensor-level signals, all data were transformed into one common reference position. After tSSS, MEG data were visually inspected to select good quality raw data segments. Mean signal duration of accepted data was 520 s (std 130 s, range 263–609 s) DBS_{OFF}, 530 s (std 116 s, range 293–610 s) DBS_{ON}, and 260 s (std 57 s, range 168–295 s) for controls. For all subjects and conditions, the amount of data was sufficient for acquiring stable results.

2.4. Signal processing and burst extraction

Further signal processing was done using MNE-python version 0.22 (Gramfort et al., 2013). After band-pass filtering the data to 2–48 Hz with a one-pass, zero-phase, non-causal FIR filter (MNE firwin filter design using a Hamming window), power spectral analysis was carried out using Welch's method with an FFT length of 2048 (2 & 3 kHz sampling rate), 1024 (1 kHz sampling rate) or 512 (600 Hz sampling rate). Power spectral density was plotted topographically for all channels. Plots were visually inspected to exclude significant remaining DBS artefacts after preprocessing.

The subsequent analysis steps are shown schematically in Fig. 1. We defined a region of interest (ROI) of three gradiometer channel pairs per hemisphere that showed a prominent signal. From these, we manually selected the gradiometer channel with the biggest beta signal peak (during the DBS_{OFF} condition in patients) and extracted all subjects' individual peak beta frequency band in the range of 12–30 Hz for both hemispheres. Individual frequency band could vary in width, depending on the width of the individual beta peak. If there was more than one beta range peak, the one with the lowest frequency was chosen, similarly to (Tinkhauser et al., 2017b). The mean ± std peak frequencies are depicted in Table 2. The selected channel (one per hemisphere) was used for further burst analysis.

Burst extraction was carried out as described by Tinkhauser et al. (2017b). Data were downsampled to 200 Hz, high-pass filtered at 2 Hz and decomposed by convolving the signal with a set of complex Morlet wavelets over the frequency range of 7–47 Hz with 1 Hz resolution and n_cycles=frequency/2. Signal was averaged across the individual peak (see Table 2) beta frequency band (± 2–3 Hz around the peak based on visual inspection). The band-pass filtered beta amplitude envelope was then thresholded at the 75th percentile amplitude for each channel and condition individually (in contrast with Tinkhauser et al. (2017b) where a common amplitude threshold was used). All periods exceeding this threshold for 100 ms or longer were defined as beta bursts. Average burst duration, average maximum burst amplitude, and bursts per second (burst rate) were calculated per hemisphere for all subjects.

Next, we assessed whether bursting patterns, i.e., the timing of burst events with respect to each other, differ between subject groups and conditions. In single-cell activity analysis, inter-spike intervals can be used to classify spiking behavior. Analogously, we here defined beta bursts as events and investigated inter-bursts as amenable to methods used for spike pattern analysis.

To estimate the variation of inter-spike intervals, we calculated the coefficient C_V proposed by Shinomoto et al. (2005), defined as the waiting times' standard deviation σ, divided by their mean μ:

$$C_V = \frac{\sigma}{\mu}$$

For a series of intervals between events which are independently exponentially distributed, C_V takes a value of 1 provided the number of observations is sufficiently large. For an entirely regular event sequence with constant intervals between events, C_V will be 0. If C_V is larger than 1, a dataset is said to be over-dispersed, pointing to the existence of clusters of occurrences. A distribution's dispersion can also be referred to as the dispersion index D which is the term we use here.

To explore burst patterns further, we assessed the probability of further bursting occurring after each burst. To this end, the time series were binarized into bursting and non-bursting times as described above. Using burst offsets as events, the 30 s following each burst were extracted and mean burst probability was calculated across all post-burst epochs. We looked at (a) bursts following a burst, (b) bursts following a long burst (> 200 ms), and (c) bursts following a short burst (100–200 ms). Individual mean time series were smoothed with a Gaussian kernel with FWHM=1 s using SciPy and divided by corresponding baseline burst rate for the whole time series, resulting in three curves. For visualization purposes, the curves were smoothed again with a Gaussian kernel (FWHM=1 s).

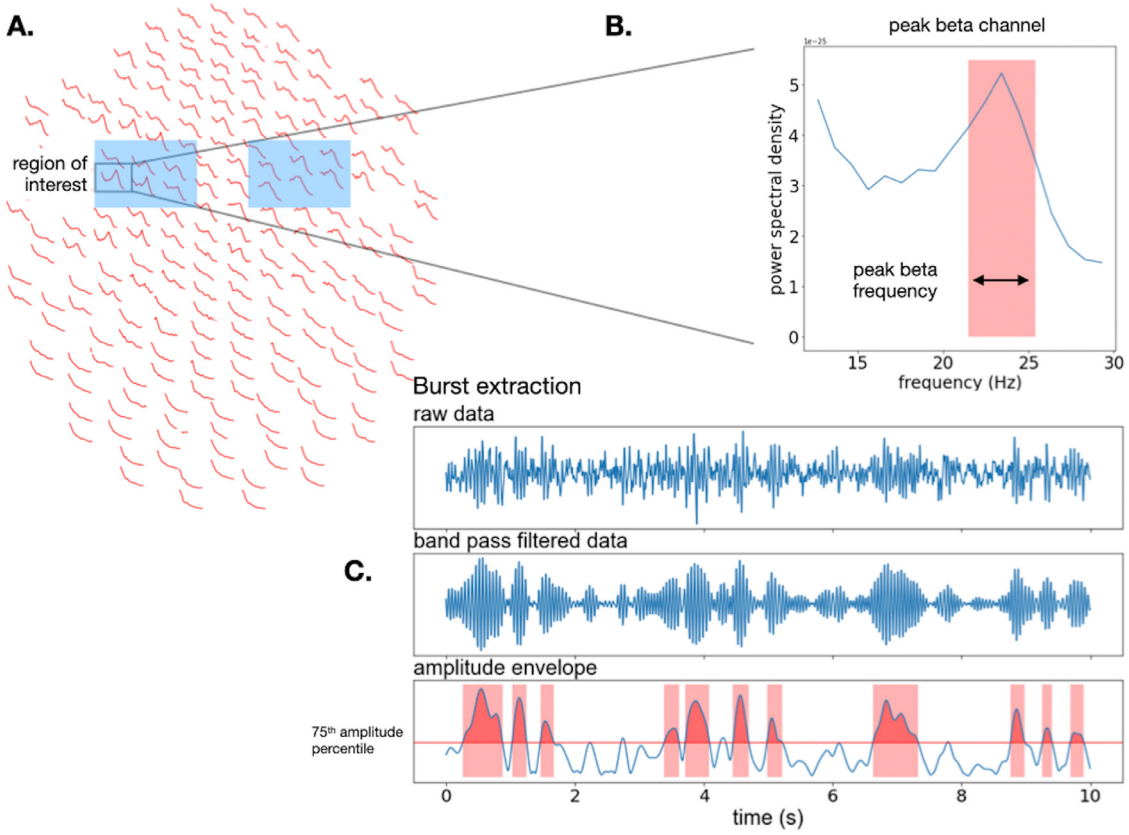

Fig. 1. Schematic illustrating beta burst analysis. (A) Regions of interest consisting of three gradiometer channel pairs were selected over the motor cortex in both hemispheres. (B) Signals were band-pass filtered at 12–30 Hz, and beta peak frequencies were individually determined. (C) Beta range bursts were extracted, averaged across the peak frequency band, and amplitude thresholded at 75th percentile.

2.5. Statistics

Statistical testing was carried out in Python using SciPy and Pingouin (Vallat, 2018). Group matching was tested using an independent samples *t*-test for age, and a chi squared test for the nominal data (gender, handedness). Bursting characteristics were compared at the hemisphere level. After testing for normality of distribution, group differences in bursting parameters (burst duration, burst amplitude, burst rate and inter-burst interval (IBI) dispersion between controls and PD patients were tested using independent samples tests (independent samples *t*-test or Mann-Whitney test). DBS ON vs. OFF conditions were compared using dependent samples tests (dependent samples *t*-test or Wilcoxon signed-rank test). The test used is indicated in the Results section. The distribution of burst durations for DBS_{ON} vs. DBS_{OFF} was compared using a two-way repeated measures ANOVA (5 × 2 design: 5 burst duration bins, 2 DBS conditions), and a mixed model ANOVA (patients vs. controls, 5 × 2 design, within-subject factor burst duration, between-subject factor group). Normal distribution was assessed visually via a Q-Q plot, and post-hoc testing was carried out using pairwise t-tests in Pingouin. Correlation between clinical scores and burst characteristics was assessed using Spearman's Rank Order correlation. To control for multiple comparisons, we carried out a False Discovery Rate correction (Benjamini and Hochberg, 1995).

To assess whether the re-burst probability following a burst was significantly different from baseline over time, data was averaged per hemisphere in successive 1-s windows and a one-sample *t*-test was used to check whether the distribution was significantly greater than 1 (baseline burst probability). Time periods of 2 s or longer (2 contingent 1-s intervals) were considered significant. To compare re-burst probabilities across different groups and bursting conditions, the individual peak within 1–2 s of post burst-offset was extracted, and peaks were compared using a paired (ON vs. OFF DBS, long vs. short bursts) or independent samples (DBS ON/OFF vs. control) *t*-test.

Data cannot be made publicly available due to Finnish data protection law. Data can, however, be shared for research collaboration with an amendment to the research ethics permit via the hospital's ethics committee, and a related data transfer agreement. All analysis code is available under https://github.com/BioMag/dbs_pd_beta_burst.

3. Results

3.1. Motor cortical beta bursting is modulated by DBS

Fig. 2 illustrates how burst duration, burst rate and amplitude were modulated by DBS. Compared to DBS_{OFF}, burst duration was shorter for DBS_{ON} (medians 213 ms DBS_{OFF} and 203 ms DBS_{ON}, Wilcoxon test, $Z = 39.0$, $p < 0.001$) and burst amplitude lower (medians DBS_{OFF} 2.6×10^{-11} T/cm, DBS_{ON} 2.4×10^{-11} T/cm, paired-samples *t*-test, $t = 2.4$, $p = 0.025$). Burst rate was higher for DBS_{ON} than DBS_{OFF} (mean DBS_{OFF} 1.03/s, DBS_{ON} 1.07/s, Wilcoxon test, $Z = 81.0$, $p = 0.002$). Thus, patients had fewer bursts which were longer in duration and higher in amplitude during DBS_{OFF} compared to the DBS_{ON} condition.

The DBS_{ON} condition in PD patients resembled the healthy control state. While burst duration and amplitude differed significantly between the DBS_{OFF} condition and controls (*burst duration:* $p = 0.002$; *amplitude:* $p = 0.001$), only amplitude was significantly different between DBS_{ON} and controls ($p = 0.027$).

3.2. Longer bursts are reduced during DBS_{ON} in favor of shorter bursts

To elucidate what drives the difference in mean burst duration between conditions, burst duration distribution was further investigated

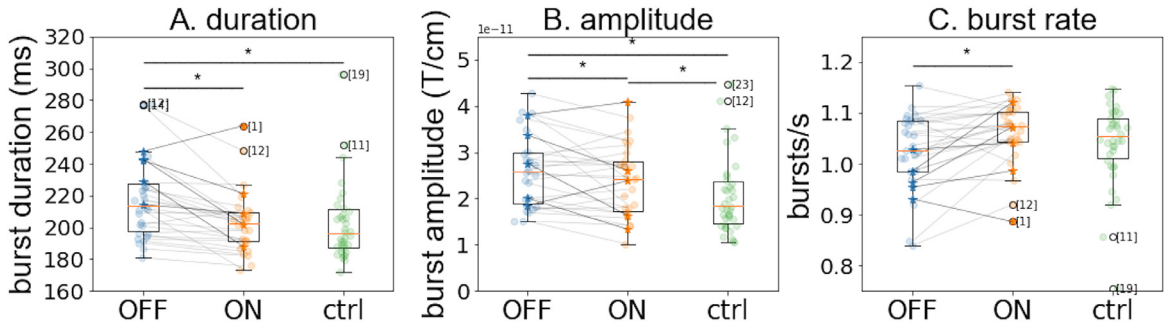

Fig. 2. Motor cortical beta bursting characteristics for DBS_{OFF} (blue) vs. DBS_{ON} (orange) vs. control subjects (green) shown as Tukey box-and-whisker plot. Boxes extend from the lower to upper quartile values, with a red line at the median. Whiskers show the last value inside 1.5 x interquartile range below the 1st and above the 3rd quartile, black circles indicate outliers (annotated with hemisphere id). Colored dots are overlayed to indicate individual data points and gray lines connect DBS_{OFF} and DBS_{ON} pairs. The darker lines and dots indicate data from the three subjects (5 hemispheres) measured while ON medication. Mean bursting duration (A), mean burst amplitude (B), and mean burst rate (C) were all significantly different for DBS_{OFF} vs. DBS_{ON} (*burst duration:* $p<0.001$; *burst amplitude:* $p = 0.025$; *burst rate:* $p = 0.002$).

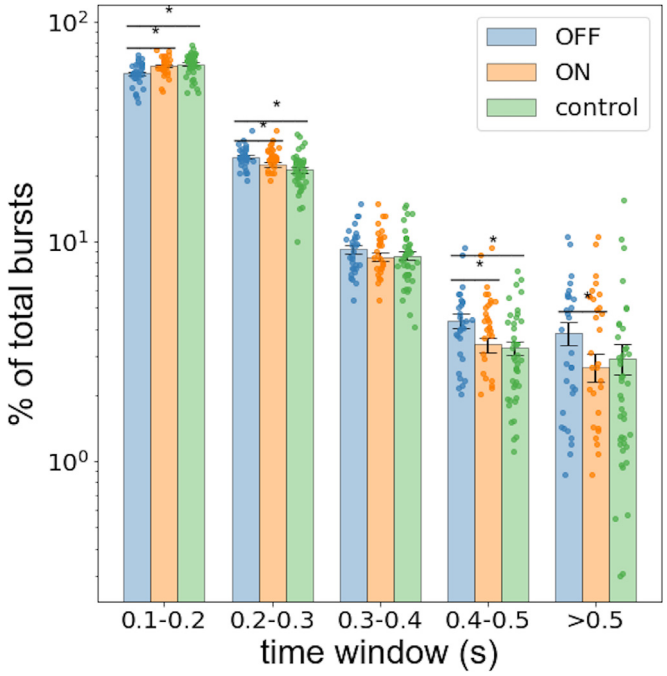

Fig. 3. Burst duration distribution for DBS_{OFF} (blue), DBS_{ON} (orange), and control subjects (green). Colored dots are overlayed to indicate individual data points. There were significantly more long bursts during DBS_{OFF} than DBS_{ON} or in controls (interaction between burst duration bin and group for DBS_{OFF} vs. DBS_{ON} ($F = 18.6$, $p<0.001$), and DBS_{OFF} vs. control ($F = 9.8$, $p<0.001$). Asterisks mark the significant differences between conditions. Note that the y-axis scale is logarithmic.

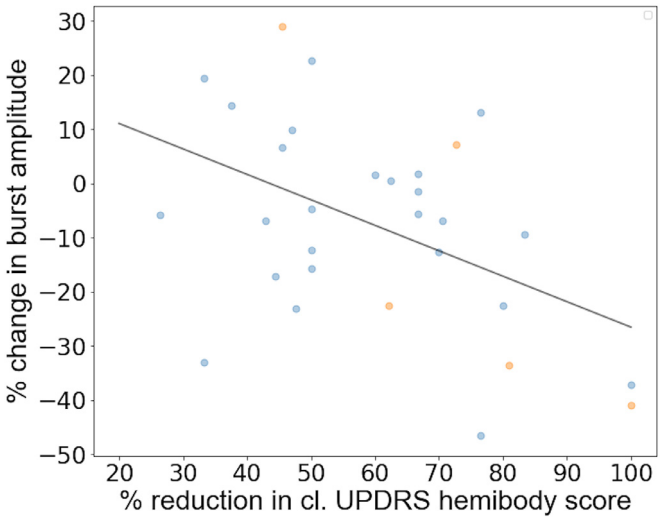

Fig. 4. DBS-induced bursting changes are related to clinical improvement. Bigger reductions in beta burst amplitude over the motor cortex were associated with stronger reduction in clinical symptoms (UPDRS hemibody score; Spearman's rank-order correlation, rho = −0.42, $p = 0.02$). Patients measured OFF medication are shown in blue, whereas patients measured ON medication are shown in orange. Removing the subjects measured ON medication rendered the correlation insignificant (Spearman's rho = −0.28, $p = 0.18$).

(see Fig. 3). Two-way repeated measures ANOVA showed a significant interaction between DBS condition and burst duration bin (two-way, repeated measures ANOVA, $F = 18.6$, $p<0.001$). Post-hoc testing demonstrated significantly more short bursts for DBS_{ON} (0.1–0.2 s), and significantly more long bursts for DBS_{OFF} (bins of 0.2–0.3 s, 0.4–0.5 s and >0.5 s). Thus, DBS reduces the number of long bursts in favor of shorter bursts.

3.3. Clinical improvement is correlated with the beta burst amplitude changes

DBS induces changes in bursting parameters, but is the magnitude of these changes reflected in changes in clinical parameters? Fig. 4 shows a scatter plot of change in burst amplitude against reduction in contralateral UPDRS III hemibody score (items 20–26). In patients, changes in beta burst amplitude for DBS_{OFF} vs. DBS_{ON} correlated with reductions in the clinical symptoms (Spearman's rho = −0.42, $p = 0.02$, see Fig. 4): Bigger reduction in burst amplitude was associated with bigger reductions in clinical symptoms of the contralateral side. The relationship between burst duration and UPDRS III hemibody score was not significant.

3.4. DBS normalizes beta bursting characteristics

We next compared the bursting patterns of PD patients to healthy, age-matched controls. While burst duration and amplitude differed significantly between the DBS_{OFF} condition (patients) and controls (Fig. 2, *burst duration*: Mann-Whitney U test, median DBS_{OFF} 213 ms, controls 196 ms, $U = 381.0$, $p = 0.002$; *amplitude*: Mann-Whitney U test, median DBS_{OFF} 2.6×10^{-11} T/cm, controls 1.9×10^{-11} T/cm $U = 365.0$, $p = 0.001$), only amplitude was significantly different between DBS_{ON} (patients) and controls (Fig. 2, *burst amplitude*: Mann-Whitney *U* test,

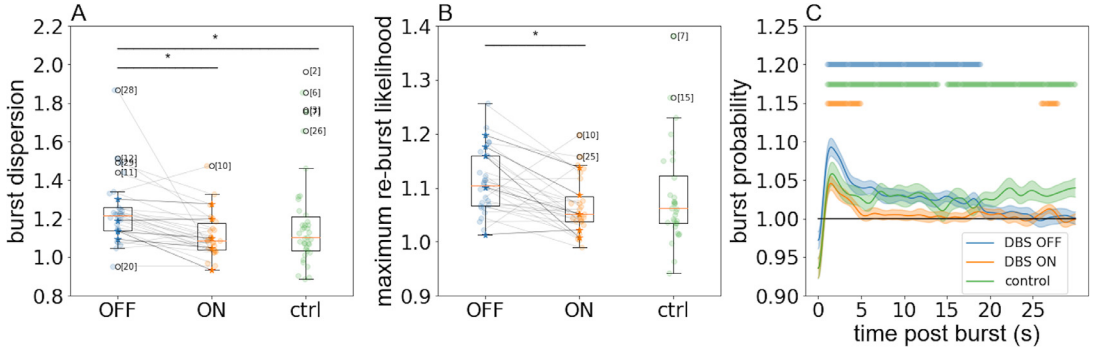

Fig. 5. A. Inter-burst intervals are over-dispersed in the DBSOFF condition compared to DBSON condition (p<0.001), and controls (p = 0.006). B. Peak re-burst likelihood is higher DBSOFF compared to DBSON (p<0.001). Lines connect individual data sets' DBSON and DBSOFF condition; Darker lines and dots indicate data for the three subjects (5 hemispheres) measured ON medication. C. Burst likelihood is elevated for a prolonged period following the end of a burst. Burst likelihoods are shown for the different groups (DBSOFF (blue), DBSON (orange), control subjects (green)). Lines at the top indicate times when burst likelihood is significantly elevated compared to baseline. Note that in C, the line does not originate from 0 due to smoothing (Gaussian smoothing kernel with FWHM of 1 s).

median DBS_{ON} 2.4 × 10^{-11} T/cm, control 1.9 × 10^{-11} T/cm, U = 461, p = 0.027).

Similarly, mixed-models ANOVA comparing burst duration distribution for DBS_{OFF} and controls showed a significant interaction between group and burst duration bin (F = 9.8, p<0.001, Fig. 3), with significantly more long bursts (0.2–0.3 s, 0.4–0.5 s) and significantly fewer short bursts (0.1–0.2 s) for DBS_{OFF} bursts on post-hoc testing. The same comparison for DBS_{ON} and controls was not significant. Thus, the DBS_{ON} condition resembled the healthy control state in several of the burst characteristics.

3.5. *Bursting activity is more clustered and re-bursting probability increased in DBS_{OFF}*

Finally, we addressed the question whether the changes in bursts' parameters described above are related to how the bursting is patterned. Fig. 5A shows the inter-burst interval (IBI) dispersion coefficient D for patients and controls. There was a significant difference in IBI dispersion between groups: the dispersion index was highest for DBS_{OFF} (DBS_{OFF} vs. DBS_{ON}: Wilcoxon test, Z = 35.0, p = 4.9 × 10^{-5}; DBS_{OFF} vs. control: Mann-Whitney U test, mean DBS_{OFF} = 1.23, control = 1.18, u = 412.0, p = 0.006), suggesting the occurrence of burst event clusters in the DBS_{OFF} condition. There was no significant difference between DBS_{ON} and controls.

We further explored the pattern of bursting by asking how the likelihood of further bursting is affected by the fact that a burst occurred. Fig. 5B shows the peak re-burst likelihood, and Fig. 5C illustrates the re-burst probability following a burst over time. *Re*-burst likelihood is increased in all groups and conditions (peak means DBS_{OFF} 1.1, DBS_{ON} 1.07, control 1.1). The duration of elevated re-burst likelihood differs between conditions, being longest for controls (28 s), and shortest for DBS_{ON} (5 s). *Re*-burst probability is highest for DBS_{OFF} and significantly different from DBS_{ON} (paired samples t-test, t = 4.0, p<0.001), whereas DBS_{OFF} vs. controls and DBS_{ON} vs. controls did not differ significantly.

3.6. *Further bursts are more likely after long beta bursts*

If the burst probability is increased after a burst, are there differences for different types of bursts? Fig. 6 shows the re-burst likelihood following long (>200 ms) versus short (100–200 ms) bursts for the different groups and conditions (Fig. 6A-C). Long bursts are more likely to be followed by bursts than short bursts for all conditions (Fig. 6D, DBS_{OFF}, Wilcoxon test, Z = 81.0, p = 0.002; DBS_{ON}, Wilcoxon test, Z = 15.0, p<0.001; controls, Wilcoxon test, Z = 90.0, p<0.001). Whereas for DBS_{OFF}, the re-burst likelihood remains elevated for a while and then returns to baseline, it quickly returns to baseline level for DBS_{ON}. In controls, re-burst likelihood is elevated for longest of all, pointing to differences in bursting patterns between patients and control subjects irrespective of DBS (Fig. 6A-C).

The dispersion coefficient analysis revealed rather large variability within the control group. We thus repeated the re-burst analysis removing three individuals (6 hemispheres). *Re*-burst likelihood was still elevated in a sustained manner in controls (Supplementary Fig. 1b). Peak re-burst probability DBS_{OFF} was now significantly different from both DBS_{ON} and controls, whereas DBS_{ON} and control still did not differ significantly from each other (Medians: DBS_{OFF}: 1.11, DBS_{ON}: 1.05, controls: 1.06; comparison ON vs. OFF, Wilcoxon test, t = 68.0, p<0.001, ON vs. ctrl, Mann Whitney test, U = 533.0, p = 0.47, OFF vs. ctrl, Mann Whitney test, U = 322.0, p = 0.003, Supplementary Fig. 1c). Comparing long and short bursts, re-burst likelihood was transiently elevated immediately after the long bursts as before, whereas following short bursts, there was now a delayed and still prolonged increase in re-burst likelihood (Supplementary Fig. 2a-c). The other results did not change qualitatively.

Since 3 patients were measured ON medication, the analyses were repeated also by excluding these 3 patients (altogether 5 hemispheres). Excluding these subjects affected the amplitude results: Burst amplitude DBS_{OFF} vs. DBS_{ON} became non-significant (p = 0.086), as well as DBS_{ON} vs. control (p = 0.053). The correlation between change in beta burst amplitude DBS_{OFF} vs. DBS_{ON} and reductions in the clinical symptoms also became non-significant (Spearman's rho = −0.28, p = 0.18). The other results were unaffected. Data from the individuals on medication has been visualized separately in the plots.

3.7. *Effect of analysis parameters*

To test stability of the results across a range of parameters, we carried out the above analysis with burst amplitude percentile thresholds varying from 50th to 90th percentile (in steps of 10). For the cut-off values in the 50th to 80th percentile range, all results remained significant except for some post-hoc comparisons for burst duration distribution. Furthermore, lowering the burst duration limit (50 and 75 ms) did not alter results. In addition, burst rate difference DBS_{OFF} vs. control became significant for both 50 and 75 ms duration limits.

In summary, we here demonstrate that DBS-induced changes in Parkinson's disease can be demonstrated in the primary motor cortex using MEG. Furthermore, individual beta burst characteristics resemble controls' findings during DBS_{ON}, whereas the patterning of beta bursting still appears to differ between groups. A summary of cardinal beta bursting features can be found in Table 3.

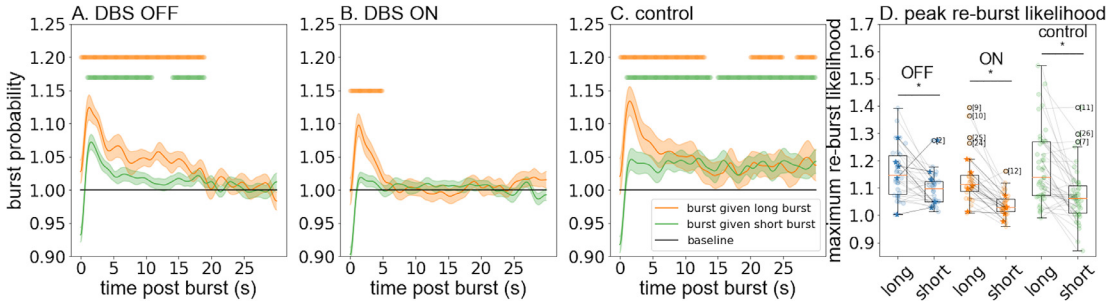

Fig. 6. Burst likelihood following long (>200 ms) bursts (orange) and short bursts (100–200 ms, green) for DBSOFF (A), DBSON (B) and controls (C). The shaded areas indicate +/- 1 SEM, the bars at the top indicate time periods for which the re-burst likelihood is significantly elevated over baseline. (D) Peak re-burst likelihood differed between long and short bursts for all conditions (long vs. short: DBSOFF, $p = 0.002$; DBSON, $p<0.001$; controls, $p<0.001$). Again, lines connect individual data sets in different conditions, and darker lines and dots indicate data for the three PD patients (5 hemispheres) measured ON medication.

Table 3
Motor cortical beta bursting characteristics comparison across groups.

		DBS_{OFF}	DBS_{ON}	Control
Burst characteristic	amplitude	high	intermediate	low
	duration	long	short	short
	rate	low	high	high
Burst patterning	dispersion	over-dispersed		
	re-burst probability	high	lower	intermediate-high
	duration of elevated re-burst probability	prolonged	transient	sustained?
	difference short vs. long bursts	similar	re-burst probability long > short	long bursts are clustered, short bursts sustained

4. Discussion

Our results recapitulate, for cortical brain activity, the previous findings of increased beta burst duration and amplitude in PD patients in STN (Tinkhauser et al., 2017b) and GPi (Eisinger et al., 2020), and a modulatory effect of STN DBS on the amplitude of beta bursts (Tinkhauser et al., 2017a). Furthermore, the results confirm the lower rate of cortical beta bursts in patients OFF therapy (STN-DBS) compared to controls, demonstrated previously in medication OFF condition (Vinding et al., 2020). The present results critically extend previous findings in that we directly compared PD patients with healthy controls, demonstrating that STN DBS significantly reduces spontaneous cortical beta burst duration and amplitude, and increases burst rates, making them more like those of healthy controls. Finally, we demonstrate, for the first time, significant changes in the higher-level patterning of beta bursting, i.e., in the clustering of bursts and in re-burst probability irrespective of DBS.

4.1. Correlation between beta bursting and symptom severity

While STN beta power and bursting are correlated with clinical symptoms and their modulation by therapy (Haumesser et al., 2021; Lofredi et al., 2019; Neumann et al., 2016; Tinkhauser et al., 2017b), the relationship between cortical beta power and/or burst characteristics and clinical symptoms in PD has remained less clear. We here find a relationship between change in bursting characteristics with DBS and the magnitude of clinical impairment.

Beta power in contralateral sensorimotor cortex has been shown to relate to the speed of hand motion in PD (Tamas et al., 2019a), and phase-amplitude coupling between beta and gamma bands to bradykinesia severity (Malekmohammadi et al., 2018). The spontaneous burst rate has also been observed to be commensurate with bradykinesia in PD patients (Vinding et al., 2020). However, while the strength of synchronization between STN and cortex appeared to be related to clinical symptoms, motor cortical beta bursting was not found to be correlated with clinical parameters in the same study (Tinkhauser et al., 2018), a result paralleled by a rodent model of PD (Haumesser et al., 2021). The relationship between cortical beta oscillatory activity and behavioral parameters is probably weaker than for STN, and thus, variable results between studies could be due to the differing cohort sizes and variability naturally inherent to the behavioral parameters used.

4.2. Beta bursting in the healthy brain

Cortical beta oscillations and their coordination/synchronization across brain regions are implicated in many brain processes, such as sensory perception, selective attention, and motor planning and initiation (Bauer et al., 2006; Jones et al., 2010; Parkkonen et al., 2015; Sacchet et al., 2015; Siegel et al., 2008; Van Ede et al., 2011). The timing of individual transient beta burst events is related to physical actions and it is different for different brain areas (Feingold et al., 2015). Furthermore, burst rate and timing predict stimulus detection (Bauer et al., 2006) and single trial behavior (Little et al., 2019). Thus, both beta burst rates and timing and their dynamic adjustment mediate healthy stimulus processing and action generation. In the healthy brain, sensorimotor beta bursting is more patterned and amplitude-modulated than that of other cortical brain areas, with higher burst amplitudes and longer burst interval times (Seedat et al., 2020).

4.3. Relevance of burst clusters

Beta bursts were over-dispersed, *i.e.*, more clustered in the untreated (DBS_{OFF}) parkinsonian state compared to both treated (DBS_{ON}) state and healthy controls. Peak re-burst probability was higher DBS_{OFF} vs. DBS_{ON}, but more sustained for controls than for PD patients both DBS_{ON} and DBS_{OFF}. The burst clustering suggests an underlying, lower-frequency oscillatory state which facilitates formation of trains of beta-frequency bursts. On the other hand, healthy controls' beta bursts were less clustered, meaning that individual beta bursts are more independent from each other in healthy subjects than in PD patients. Short bursts

were associated with lower peak re-burst probabilities than long bursts, i.e. they were less likely to occur in trains of bursts. It has been hypothesized that prolonged beta bursts, which are associated with increased network synchrony in the beta range, 'jam' the information coding capacity of the underlying oscillating brain network (Hammond et al., 2007). Burst clustering suggests that even between individual beta bursts, the network is at an increased state of readiness to produce further beta oscillatory bursts, and thus unable to 'shift set' by suppressing beta frequency activity dynamically, as may be necessary when generating movements (Little et al., 2019) or process stimuli successfully (Shin et al., 2017).

The change between DBS_{OFF} and DBS_{ON} conditions in the median burst duration was small, ~10 ms, and may not be clinically relevant. Instead, the tail of the burst duration distribution (*i.e.*, the occurrence of very long bursts), and elevated re-bursting probability (burst clustering) are probably physiologically more relevant phenomena: If the state of the system favours prolonged and repeated bursting, it will probably be more difficult to be suppressed when needed. Interestingly, our findings also suggest that during DBS_{OFF} there were more mid-range (0.2–0.4 s) bursts than during DBS_{ON}, explaining why the median differences between conditions remained small, further suggesting that the tails of the distribution could provide clinically more relevant information.

Somewhat surprisingly, the re-bursting probability behavior in DBS_{ON} condition was different from the data of normal controls. *Re*-burst probability DBS_{ON}, especially for short bursts, carried less information about the temporal structure of further bursts than both DBS_{OFF} condition and the data in normal controls. It is known that STN-DBS induces subtle behavioural changes in the subjects, e.g., proneness to rash and impulsive mistakes in a Go/No-go motor task (Ballinger et al. 2009). It could be that the reduced temporal correlation between bursts in DBS_{ON} is a manifestation of reduced inhibitory effect of the basal ganglia loop on sensorimotor cortex.

4.4. Cortical beta bursting and beta oscillatory network

The observed changes in PD patients' cortical beta burst parameters compared to controls and their modulation by STN DBS are consistent with existing literature. Previous studies have demonstrated increased beta band sensorimotor cortical power in PD patients ((Hall et al., 2014; Pollok et al., 2012; Whitmer et al., 2012), but see also (Heinrichs-Graham et al., 2014)) and in rodent models of PD (Brazhnik et al., 2012; Degos et al., 2009; Haumesser et al., 2021; Jávor-Duray et al., 2017; Sharott et al., 2005). Furthermore, several studies have shown increased synchronization in the beta band between STN and motor cortical regions in humans (Cagnan et al., 2019; Oswal et al., 2016; Tinkhauser et al., 2018), primates (Yu et al., 2021) and rodents (Cagnan et al., 2019; Sharott et al., 2005), also implying motor cortical beta band activity.

4.5. Oscillatory network modulation by DBS

As outlined earlier, STN beta bursting in PD arises from the pathological entrainment of STN neurons by cortical beta oscillations, giving rise to a pathological oscillatory network encompassing the subthalamic nucleus, basal ganglia, and cortex. This is evidenced by pathological beta oscillatory activity in several of the network nodes (Abbasi et al., 2018; Eisinger et al., 2020; Tamas et al., 2019a, 2019b). STN DBS has previously been shown to suppress beta band activity in the sensorimotor cortex (Abbasi et al., 2018; Tamas et al., 2019b, 2019a). Clinically, disruption of oscillatory beta activity by both STN-DBS as well as DBS of the globus pallidus alleviates PD motor symptoms (Follett et al., 2010). The beta band activity reduction for DBS at the sensorimotor cortex is an reflection of the reduced activity in the cortico-subcortical oscillatory network. While beta oscillations still occur, the network is less likely to remain locked in the beta oscillatory state for prolonged (bursts) and repeated periods of time (burst clusters), as is the case when the cortex and subcortical structures are pathologically locked in synchrony.

4.6. Relevance for adaptive DBS

Much progress has been made in developing adaptive DBS (aDBS) to tailor stimulation towards patients' individual and dynamically changing needs, with the intention of further improving symptom alleviation and reducing the amount of DBS-related side effects. One approach is the local STN sensing option that utilizes different beta oscillatory band signal features and temporal dynamics, such as instantaneous (< 1 s) beta band amplitude (Little et al., 2013; Piña-Fuentes et al., 2020; Velisar et al., 2019), slower (minute range) beta band activity level fluctuations (Arlotti et al., 2018; Rosa et al., 2017), or stimulation at specific phases of the beta band activity (Holt et al., 2019). Cortical sensing of gamma band activity has also been investigated (Swann et al., 2018). Preliminary short-term studies show improved side effect profiles (Piña-Fuentes et al., 2020; Swann et al., 2018), but data on chronic effects are lacking. Our current results show that (long) beta bursts do not occur independently from each other. Thus, measures of the individual clustering of beta bursts may be a useful additional biomarker for tailoring adaptive DBS paradigms to combine the fast adaptive beta amplitude control mechanism and the more sluggish, time-integrated overall beta band activity.

Furthermore, we show that while most beta bursts in healthy controls' motor cortex are short, long beta bursts also occur spontaneously to a varying degree. Previous studies of healthy brain function have focused primarily on beta burst timings and rates, and less on the characteristics of individual bursts. Whether or not individual cortical beta burst duration at rest and during different task-specific processing is relevant to how a stimulus is processed in the healthy brain should be addressed in future studies, to further understand beta bursts' functional relevance.

4.7. Relevance of beta frequency sub-bands

In the present study, we concentrated on the beta peak frequency, based on previous data using similar approach for STN (Tinkhauser et al., 2017a), to establish whether the findings could be replicated with non-invasive measurements of the sensorimotor cortex. The different beta band peaks probably correlate with different components of the motor system network. While the lower beta frequency peak is believed to be a manifestation of oscillations in the subthalamic-basal ganglia-cortical loop, there is evidence suggesting that STN-cortex coupling in the high beta frequency band is the electrophysiological manifestation of the hyper-direct pathway. Low beta activity is significantly higher in untreated PD patients and can be suppressed after dopamine medication (López-Azcárate et al., 2010; Oswal et al., 2016; but see also Sure et al., 2021). Also, clinical parkinsonian signs were concomitant with power increases in low beta band (12–18 Hz, Florin et al., 2013; Steiner et al., 2017; but see also Sure et al., 2021). On the other hand, coupling delays between the STN and motor cortex were shorter in the high beta band than in the low beta band (Ozturk et al., 2020). Also, the STN-premotor coherence at the high beta band significantly correlates with the STN-cortex fiber tract densities (Oswal et al., 2021), suggesting that the high beta band may represent activity in the hyperdirect pathway, which is preserved in Parkinson's disease. The pathologically synchronous oscillatory activity in the network appears to occur at the lower beta frequencies (Oswal et al., 2021).

4.8. Limitations

The analysis presented here was carried out at the channel level, not at the source level. The ROI was chosen over frontal motor areas and within this ROI, the individual peak beta activity channel was chosen for characterizing sensorimotor rhythmicity. As the anatomical location

of the sensorimotor cortex is very constant across individuals, the ROI channels should very well capture the sensorimotor beta rhythm in all patients. Still, possible confounds of several sources contributing to the beta activity visible at the channel level cannot be fully excluded. However, significant contribution of deep sources at the cortical level is unlikely.

DBS generates large electromagnetic artefacts which contaminate the MEG data due to both the applied current and the movement of wires connecting the stimulator with the electrode. Both MEG data acquisition and preprocessing were optimized to minimize DBS-related noise. Kandemir et al. compared several interference suppression approaches for MEG data of DBS patients, demonstrating that tSSS, the noise suppression algorithm used here, showed good results at the sensor and source level (Kandemir et al., 2020). Data segments with excessive remaining noise were excluded from further analysis. Nevertheless, signal-to-noise ratio may be lower in the DBS_{ON} condition, but this is unlikely to affect the present results.

5. Conclusion

Cortical sensorimotor beta bursting in PD patients differs from healthy controls' bursting activity in burst duration, rate, amplitude, and patterning. Conventional STN DBS makes cortical sensorimotor beta bursting in PD patients more like that of age-matched healthy controls. Furthermore, the extent of the STN DBS elicited change in beta bursting relates to changes in clinical symptoms.

Studying these therapeutic effects of DBS with MEG allows the direct comparison between PD patients and healthy controls, facilitating deeper understanding of the role of beta bursting and underlying oscillatory network in Parkinson's disease, and their possible future use as biomarkers for treatment and disease follow-up.

Data and code availability statement

Finnish data protection laws do not allow for patient MEG data to be made publicly available, as the data cannot be fully anonymized. Data sharing requires an amendment to the research ethics permit via the hospital's ethics committee, and a data transfer agreement. Analysis was carried out using standard software packages as outlined in the methods section. Scripts used to produce the results and figures presented in the study are published on the BioMag Gitlab page (https://github.com/BioMag/dbs_pd_beta_burst).

Ethics statement

This work was carried out in accordance with The Code of Ethics of the World Medical Association (Declaration of Helsinki) for experiments involving humans. All studies were approved by Helsinki University Hospital or Aalto University Ethical Committees, and all participants gave their written informed consent to participate.

Declaration of Competing Interest

Jukka Nenonen is employed by MEGIN Oy, the producer of the MEG device used for measurements. Eero Pekkonen has received lecturing fees from Abbott, the producer of the DBS stimulation device, and is the Finnish PI for the 'Abbott DBS Registry of Outcomes for Indications over Time'. Apart from that, the authors declare no other potential competing interests.

Credit authorship contribution statement

K. Amande M. Pauls: Conceptualization, Methodology, Investigation, Software, Formal analysis, Data curation, Writing – original draft. **Olesia Korsun:** Investigation, Formal analysis, Validation, Data curation, Writing – review & editing. **Jukka Nenonen:** Formal analysis, Software, Writing – review & editing. **Jussi Nurminen:** Software, Writing – review & editing. **Mia Liljeström:** Investigation, Data curation, Writing – review & editing. **Jan Kujala:** Conceptualization, Software, Methodology, Writing – review & editing. **Eero Pekkonen:** Conceptualization, Resources, Funding acquisition, Project administration, Writing – review & editing. **Hanna Renvall:** Conceptualization, Resources, Funding acquisition, Supervision, Writing – review & editing.

Funding information & role of the funding source

Amande Pauls was supported by a personal grant from the University of Helsinki. Olesia Korsun was supported by the Päivikki and Sakari Sohlberg Foundation, the Orion Research Foundation, the Finnish Parkinson Foundation and the Finnish Brain Foundation. Mia Liljeström was supported by the Swedish Cultural Foundation in Finland, the Päivikki and Sakari Sohlberg Foundation, and the Finnish Cultural Foundation. Eero Pekkonen was supported by Finnish Government research funding (TYH- fund). Hanna Renvall was supported by the Academy of Finland (grant number 321460) and Paulo Foundation.

Supplementary materials

Supplementary material associated with this article can be found, in the online version, at doi:10.1016/j.neuroimage.2022.119308.

References

Abbasi, O., Hirschmann, J., Storzer, L., Özkurt, T.E., Elben, S., Vesper, J., Wojtecki, L., Schmitz, G., Schnitzler, A., Butz, M., 2018. Unilateral deep brain stimulation suppresses alpha and beta oscillations in sensorimotor cortices. Neuroimage 174. doi:10.1016/j.neuroimage.2018.03.026.

Arlotti, M., Marceglia, S., Foffani, G., Volkmann, J., Lozano, A.M., Moro, E., Cogiamanian, F., Prenassi, M., Bocci, T., Cortese, F., Rampini, P., Barbieri, S., Priori, A., 2018. Eight-hours adaptive deep brain stimulation in patients with Parkinson disease. Neurology 90. doi:10.1212/WNL.0000000000005121.

Baaske, M.K., Kormann, E., Holt, A.B., Gulberti, A., McNamara, C.G., Pötter-Nerger, M., Westphal, M., Engel, A.K., Hamel, W., Brown, P., Moll, C.K.E., Sharott, A., 2020. Parkinson's disease uncovers an underlying sensitivity of subthalamic nucleus neurons to beta-frequency cortical input in vivo. Neurobiol. Dis. 146. doi:10.1016/j.nbd.2020.105119.

Bauer, M., Oostenveld, R., Peeters, M., Fries, P., 2006. Tactile spatial attention enhances gamma-band activity in somatosensory cortex and reduces low-frequency activity in parieto-occipital areas. J. Neurosci. 26. doi:10.1523/JNEUROSCI.5228-04.2006.

Benjamini, Y., Hochberg, Y., 1995. Benjamini Y, Hochberg Y. Controlling the false discovery rate–A practical and powerful approach to multiple testing. J. R. Stat. Soc. Ser. B. 1995:p. 289–300. J. R. Stat. Soc. B 57.

Brazhnik, E., Cruz, A.V., Avila, I., Wahba, M.I., Novikov, N., Ilieva, N.M., McCoy, A.J., Gerber, C., Walters, J.R., 2012. State-dependent spike and local field synchronization between motor cortex and substantia nigra in hemiparkinsonian rats. J. Neurosci. 32. doi:10.1523/JNEUROSCI.0943-12.2012.

Brown, P., Oliviero, A., Mazzone, P., Insola, A., Tonali, P., Di Lazzaro, V., 2001. Dopamine dependency of oscillations between subthalamic nucleus and pallidum in Parkinson's disease. J. Neurosci. 21. doi:10.1523/jneurosci.21-03-01033.2001.

Cagnan, H., Mallet, N., Moll, C.K.E., Gulberti, A., Holt, A.B., Westphal, M., Gerloff, C., Engel, A.K., Hamel, W., Magill, P.J., Brown, P., Sharott, A., 2019. Temporal evolution of beta bursts in the parkinsonian cortical and basal ganglia network. Proc. Natl. Acad. Sci. U. S. A. 116. doi:10.1073/pnas.1819975116.

Degos, B., Deniau, J.M., Chavez, M., Maurice, N., 2009. Chronic but not acute dopaminergic transmission interruption promotes a progressive increase in cortical beta frequency synchronization–Relationships to vigilance state and akinesia. Cereb. Cortex 19. doi:10.1093/cercor/bhn199.

Eisinger, R.S., Cagle, J.N., Opri, E., Alcantara, J., Cernera, S., Foote, K.D., Okun, M.S., Gunduz, A., 2020. Parkinsonian beta dynamics during rest and movement in the dorsal pallidum and subthalamic nucleus. J. Neurosci. 40. doi:10.1523/JNEUROSCI.2113-19.2020.

Feingold, J., Gibson, D.J., Depasquale, B., Graybiel, A.M., 2015. Bursts of beta oscillation differentiate postperformance activity in the striatum and motor cortex of monkeys performing movement tasks. Proc. Natl. Acad. Sci. U. S. A. 112. doi:10.1073/pnas.1517629112.

Florin, E., Erasmi, R., Reck, C., Maarouf, M., Schnitzler, A., Fink, G.R., Timmermann, L., 2013. Does increased gamma activity in patients suffering from Parkinson's disease counteract the movement inhibiting beta activity? Neuroscience 237. doi:10.1016/j.neuroscience.2013.01.051.

Follett, K.A., Weaver, F.M., Stern, M., Hur, K., Harris, C.L., Luo, P., Marks, W.J., Rothlind, J., Sagher, O., Moy, C., Pahwa, R., Burchiel, K., Hogarth, P., Lai, E.C., Duda, J.E., Holloway, K., Samii, A., Horn, S., Bronstein, J.M., Stoner, G., Starr, P.A., Simpson, R., Baltuch, G., De Salles, A., Huang, G.D., Reda, D.J., 2010. Pallidal versus subthalamic deep-brain stimulation for Parkinson's disease. N. Engl. J. Med. 362. doi:10.1056/nejmoa0907083.

Gramfort, A., Luessi, M., Larson, E., Engemann, D.A., Strohmeier, D., Brodbeck, C., Goj, R., Jas, M., Brooks, T., Parkkonen, L., Hämäläinen, M., 2013. MEG and EEG data analysis with MNE-Python. Front. Neurosci. doi:10.3389/fnins.2013.00267.

Hall, S.D., Prokic, E.J., McAllister, C.J., Ronnqvist, K.C., Williams, A.C., Yamawaki, N., Witton, C., Woodhall, G.L., Stanford, I.M., 2014. GABA-mediated changes in inter-hemispheric beta frequency activity in early-stage Parkinson's disease. Neuroscience 281. doi:10.1016/j.neuroscience.2014.09.037.

Hammond, C., Bergman, H., Brown, P., 2007. Pathological synchronization in Parkinson's disease–Networks, models and treatments. Trends Neurosci. doi:10.1016/j.tins.2007.05.004.

Haumesser, J.K., Beck, M.H., Pellegrini, F., Kühn, J., Neumann, W.J., Altschüler, J., Harnack, D., Kupsch, A., Nikulin, V.V., Kühn, A.A., van Riesen, C., 2021. Subthalamic beta oscillations correlate with dopaminergic degeneration in experimental parkinsonism. Exp. Neurol. 335. doi:10.1016/j.expneurol.2020.113513.

Heinrichs-Graham, E., Kurz, M.J., Becker, K.M., Santamaria, P.M., Gendelman, H.E., Wilson, T.W., 2014. Hypersynchrony despite pathologically reduced beta oscillations in patients with Parkinson's disease–A pharmaco-magnetoencephalography study. J. Neurophysiol. 112. doi:10.1152/jn.00383.2014.

Hirschmann, J., Özkurt, T.E., Butz, M., Homburger, M., Elben, S., Hartmann, C.J., Vesper, J., Wojtecki, L., Schnitzler, A., 2011. Distinct oscillatory STN-cortical loops revealed by simultaneous MEG and local field potential recordings in patients with Parkinson's disease. Neuroimage 55. doi:10.1016/j.neuroimage.2010.11.063.

Holt, A.B., Kormann, E., Gulberti, A., Pötter-Nerger, M., McNamara, C.G., Cagnan, H., Baaske, M.K., Little, S., Köppen, J.A., Buhmann, C., Westphal, M., Gerloff, C., Engel, A.K., Brown, P., Hamel, W., Moll, C.K.E., Sharott, A., 2019. Phase-dependent suppression of beta oscillations in Parkinson's disease patients. J. Neurosci. 39. doi:10.1523/JNEUROSCI.1913-18.2018.

Jávor-Duray, B.N., Vinck, M., van der Roest, M., Bezard, E., Berendse, H.W., Boraud, T., Voorn, P., 2017. Alterations in functional cortical hierarchy in hemiparkinsonian rats. J. Neurosci. 37. doi:10.1523/JNEUROSCI.3257-16.2017.

Jones, S.R., Kerr, C.E., Wan, Q., Pritchett, D.L., Hämäläinen, M., Moore, C.I., 2010. Cued spatial attention drives functionally relevant modulation of the mu rhythm in primary somatosensory cortex. J. Neurosci. 30. doi:10.1523/JNEUROSCI.2969-10.2010.

Kandemir, A.L., Litvak, V., Florin, E., 2020. The comparative performance of DBS artefact rejection methods for MEG recordings. Neuroimage 219. doi:10.1016/j.neuroimage.2020.117057.

Kehnemouyi, Y.M., Wilkins, K.B., Anidi, C.M., Anderson, R.W., Afzal, M.F., Bronte-Stewart, H.M., 2021. Modulation of beta bursts in subthalamic sensorimotor circuits predicts improvement in bradykinesia. Brain 144. doi:10.1093/brain/awaa394.

Kühn, A.A., Kempf, F., Brücke, C., Doyle, L.G., Martinez-Torres, I., Pogosyan, A., Trottenberg, T., Kupsch, A., Schneider, G.H., Hariz, M.I., Vandenberghe, W., Nuttin, B., Brown, P., 2008. High-frequency stimulation of the subthalamic nucleus suppresses oscillatory β activity in patients with Parkinson's disease in parallel with improvement in motor performance. J. Neurosci. 28. doi:10.1523/JNEUROSCI.0282-08.2008.

Kühn, A.A., Kupsch, A., Schneider, G.H., Brown, P., 2006. Reduction in subthalamic 8-35Hz oscillatory activity correlates with clinical improvement in Parkinson's disease. Eur. J. Neurosci. 23. doi:10.1111/j.1460-9568.2006.04717.x.

Levy, R., Ashby, P., Hutchison, W.D., Lang, A.E., Lozano, A.M., Dostrovsky, J.O., 2002. Dependence of subthalamic nucleus oscillations on movement and dopamine in Parkinson's disease. Brain 125. doi:10.1093/brain/awf128.

Little, S., Bonaiuto, J., Barnes, G., Bestmann, S., 2019. Human motor cortical beta bursts relate to movement planning and response errors. PLoS Biol. 17. doi:10.1371/journal.pbio.3000479.

Little, S., Pogosyan, A., Neal, S., Zavala, B., Zrinzo, L., Hariz, M., Foltynie, T., Limousin, P., Ashkan, K., FitzGerald, J., Green, A.L., Aziz, T.Z., Brown, P., 2013. Adaptive deep brain stimulation in advanced Parkinson disease. Ann. Neurol. 74. doi:10.1002/ana.23951.

Litvak, V., Jha, A., Eusebio, A., Oostenveld, R., Foltynie, T., Limousin, P., Zrinzo, L., Hariz, M.I., Friston, K., Brown, P., 2011. Resting oscillatory cortico-subthalamic connectivity in patients with Parkinson's disease. Brain 134. doi:10.1093/brain/awq332.

Lofredi, R., Tan, H., Neumann, W.J., Yeh, C.H., Schneider, G.H., Kühn, A.A., Brown, P., 2019. Beta bursts during continuous movements accompany the velocity decrement in Parkinson's disease patients. Neurobiol. Dis. 127. doi:10.1016/j.nbd.2019.03.013.

López-Azcárate, J., Tainta, M., Rodríguez-Oroz, M.C., Valencia, M., González, R., Guridi, J., Iriarte, J., Obeso, J.A., Artieda, J., Alegre, M., 2010. Coupling between beta and high-frequency activity in the human subthalamic nucleus may be a pathophysiological mechanism in Parkinson's disease. J. Neurosci. 30. doi:10.1523/JNEUROSCI.5459-09.2010.

Malekmohammadi, M., AuYong, N., Ricks-Oddie, J., Bordelon, Y., Pouratian, N., 2018. Pallidal deep brain stimulation modulates excessive cortical high β phase amplitude coupling in Parkinson disease. Brain Stimul. 11. doi:10.1016/j.brs.2018.01.028.

Marsden, J.F., Limousin-Dowsey, P., Ashby, P., Pollak, P., Brown, P., 2001. Subthalamic nucleus, sensorimotor cortex and muscle interrelationships in Parkinson's disease. Brain 124. doi:10.1093/brain/124.2.378.

Medvedovsky, M., Taulu, S., Bikmullina, R., Ahonen, A., Paetau, R., 2009. Fine tuning the correlation limit of spatio-temporal signal space separation for magnetoencephalography. J. Neurosci. Methods 177. doi:10.1016/j.jneumeth.2008.09.035.

Neumann, W.J., Degen, K., Schneider, G.H., Brücke, C., Huebl, J., Brown, P., Kühn, A.A., 2016. Subthalamic synchronized oscillatory activity correlates with motor impairment in patients with Parkinson's disease. Mov. Disord. 31. doi:10.1002/mds.26759.

O'Keeffe, A.B., Malekmohammadi, M., Sparks, H., Pouratian, N., 2020. Synchrony drives motor cortex beta bursting,waveform dynamics, and phase-amplitude coupling in Parkinson's disease. J. Neurosci. 40. doi:10.1523/JNEUROSCI.1996-19.2020.

Oswal, A., Beudel, M., Zrinzo, L., Limousin, P., Hariz, M., Foltynie, T., Litvak, V., Brown, P., 2016. Deep brain stimulation modulates synchrony within spatially and spectrally distinct resting state networks in Parkinson's disease. Brain 139. doi:10.1093/brain/aww048.

Oswal, A., Cao, C., Yeh, C.H., Neumann, W.J., Gratwicke, J., Akram, H., Horn, A., Li, D., Zhan, S., Zhang, C., Wang, Q., Zrinzo, L., Foltynie, T., Limousin, P., Bogacz, R., Sun, B., Husain, M., Brown, P., Litvak, V., 2021. Neural signatures of hyperdirect pathway activity in Parkinson's disease. Nat. Commun. 12. doi:10.1038/s41467-021-25366-0.

Ozturk, M., Abosch, A., Francis, D., Wu, J., Jimenez-Shahed, J., Ince, N.F., 2020. Distinct subthalamic coupling in the ON state describes motor performance in Parkinson's disease. Mov. Disord. 35. doi:10.1002/mds.27800.

Parkkonen, E., Laaksonen, K., Piitulainen, H., Parkkonen, L., Forss, N., 2015. Modulation of the ~20-Hz motor-cortex rhythm to passive movement and tactile stimulation. Brain Behav. 5. doi:10.1002/brb3.328.

Piña-Fuentes, D., van Dijk, J.M.C., van Zijl, J.C., Moes, H.R., van Laar, T., Oterdoom, D.L.M., Little, S., Brown, P., Beudel, M., 2020. Acute effects of adaptive Deep Brain Stimulation in Parkinson's disease. Brain Stimul. 13. doi:10.1016/j.brs.2020.07.016.

Piña-Fuentes, D., van Zijl, J.C., van Dijk, J.M.C., Little, S., Tinkhauser, G., Oterdoom, D.L.M., Tijssen, M.A.J., Beudel, M., 2019. The characteristics of pallidal low-frequency and beta bursts could help implementing adaptive brain stimulation in the parkinsonian and dystonic internal globus pallidus. Neurobiol. Dis. 121. doi:10.1016/j.nbd.2018.09.014.

Pollok, B., Krause, V., Martsch, W., Wach, C., Schnitzler, A., Südmeyer, M., 2012. Motor-cortical oscillations in early stages of Parkinson's disease. J. Physiol. 590. doi:10.1113/jphysiol.2012.231316.

Priori, A., Foffani, G., Pesenti, A., Tamma, F., Bianchi, A.M., Pellegrini, M., Locatelli, M., Moxon, K.A., Villani, R.M., 2004. Rhythm-specific pharmacological modulation of subthalamic activity in Parkinson's disease. Exp. Neurol. 189. doi:10.1016/j.expneurol.2004.06.001.

Ray, N.J., Jenkinson, N., Wang, S., Holland, P., Brittain, J.S., Joint, C., Stein, J.F., Aziz, T., 2008. Local field potential beta activity in the subthalamic nucleus of patients with Parkinson's disease is associated with improvements in bradykinesia after dopamine and deep brain stimulation. Exp. Neurol. 213. doi:10.1016/j.expneurol.2008.05.008.

Rosa, M., Arlotti, M., Marceglia, S., Cogiamanian, F., Ardolino, G., Fonzo, A.Di, Lopiano, L., Scelzo, E., Merola, A., Locatelli, M., Rampini, P.M., Priori, A., 2017. Adaptive deep brain stimulation controls levodopa-induced side effects in Parkinsonian patients. Mov. Disord. doi:10.1002/mds.26953.

Sacchet, M.D., LaPlante, R.A., Wan, Q., Pritchett, D.L., Lee, A.K.C., Hämäläinen, M., Moore, C.I., Kerr, C.E., Jones, S.R., 2015. Attention drives synchronization of alpha and beta rhythms between right inferior frontal and primary sensory neocortex. J. Neurosci. 35. doi:10.1523/JNEUROSCI.1292-14.2015.

Schmidt, S.L., Peters, J.J., Turner, D.A., Grill, W.M., 2020. Continuous deep brain stimulation of the subthalamic nucleus may not modulate beta bursts in patients with Parkinson's disease. Brain Stimul. 13. doi:10.1016/j.brs.2019.12.008.

Seedat, Z.A., Quinn, A.J., Vidaurre, D., Liuzzi, L., Gascoyne, L.E., Hunt, B.A.E., O'Neill, G.C., Pakenham, D.O., Mullinger, K.J., Morris, P.G., Woolrich, M.W., Brookes, M.J., 2020. The role of transient spectral 'bursts' in functional connectivity–A magnetoencephalography study. Neuroimage 209. doi:10.1016/j.neuroimage.2020.116537.

Sharott, A., Gulberti, A., Hamel, W., Köppen, J.A., Münchau, A., Buhmann, C., Pötter-Nerger, M., Westphal, M., Gerloff, C., Moll, C.K.E., Engel, A.K., 2018. Spatio-temporal dynamics of cortical drive to human subthalamic nucleus neurons in Parkinson's disease. Neurobiol. Dis. 112. doi:10.1016/j.nbd.2018.01.001.

Sharott, A., Magill, P.J., Harnack, D., Kupsch, A., Meissner, W., Brown, P., 2005. Dopamine depletion increases the power and coherence of β-oscillations in the cerebral cortex and subthalamic nucleus of the awake rat. Eur. J. Neurosci. 21. doi:10.1111/j.1460-9568.2005.03973.x.

Sherman, M.A., Lee, S., Law, R., Haegens, S., Thorn, C.A., Hämäläinen, M.S., Moore, C.I., Jones, S.R., 2016. Neural mechanisms of transient neocortical beta rhythms–Converging evidence from humans, computational modeling, monkeys, and mice. Proc. Natl. Acad. Sci. U. S. A. 113. doi:10.1073/pnas.1604135113.

Shin, H., Law, R., Tsutsui, S., Moore, C.I., Jones, S.R., 2017. The rate of transient beta frequency events predicts behavior across tasks and species. Elife 6. doi:10.7554/eLife.29086.

Shinomoto, S., Miura, K., Koyama, S., 2005. A measure of local variation of inter-spike intervals. Biosystems doi:10.1016/j.biosystems.2004.09.023.

Siegel, M., Donner, T.H., Oostenveld, R., Fries, P., Engel, A.K., 2008. Neuronal synchronization along the dorsal visual pathway reflects the focus of spatial attention. Neuron 60. doi:10.1016/j.neuron.2008.09.010.

Steiner, L.A., Neumann, W.J., Staub-Bartelt, F., Herz, D.M., Tan, H., Pogosyan, A., Kuhn, A.A., Brown, P., 2017. Subthalamic beta dynamics mirror Parkinsonian bradykinesia months after neurostimulator implantation. Mov. Disord. 32. doi:10.1002/mds.27068.

Sure, M., Vesper, J., Schnitzler, A., Florin, E., 2021. Dopaminergic modulation of spectral and spatial characteristics of Parkinsonian subthalamic nucleus beta bursts. Front. Neurosci. 15. doi:10.3389/fnins.2021.724334.

Swann, N.C., De Hemptinne, C., Thompson, M.C., Miocinovic, S., Miller, A.M., Gilron, R., Ostrem, J.L., Chizeck, H.J., Starr, P.A., 2018. Adaptive deep brain stimulation for Parkinson's disease using motor cortex sensing. J. Neural Eng. 15. doi:10.1088/1741-2552/aabc9b.

Tamas, G., Kelemen, A., Javor-Duray, B., Palotai, M., Halasz, L., Eross, L., Fekete, G., Bognar, L., Deuschl, G., Muthuraman, M., 2019a. Beta power in the primary sensorimotor cortex correlates with bradykinesia in parkinsonian patients treated with bilateral subthalamic deep brain stimulation. Neuromodulation 22.

Tamas, G., Kelemen, A., Javor-Duray, B., Palotai, M., Halasz, L., Eross, L., Fekete, G., Bognar, L., Deuschl, G., Muthuraman, M., 2019b. Low and high beta band activity in

the primary sensorimotor cortex is diminished by ipsilateral subthalamic stimulation in Parkinsonian patients. Mov. Disord. 34.

Taulu, S., Kajola, M., 2005. Presentation of electromagnetic multichannel data–The signal space separation method. J. Appl. Phys. 97. doi:10.1063/1.1935742.

Taulu, S., Simola, J., 2006. Spatiotemporal signal space separation method for rejecting nearby interference in MEG measurements. Phys. Med. Biol. 51. doi:10.1088/0031-9155/51/7/008.

Tinkhauser, G., Pogosyan, A., Little, S., Beudel, M., Herz, D.M., Tan, H., Brown, P., 2017a. The modulatory effect of adaptive deep brain stimulation on beta bursts in Parkinson's disease. Brain 140. doi:10.1093/brain/awx010.

Tinkhauser, G., Pogosyan, A., Tan, H., Herz, D.M., Kühn, A.A., Brown, P., 2017b. Beta burst dynamics in Parkinson's disease off and on dopaminergic medication. Brain 140. doi:10.1093/brain/awx252.

Tinkhauser, G., Torrecillos, F., Duclos, Y., Tan, H., Pogosyan, A., Fischer, P., Carron, R., Welter, M.L., Karachi, C., Vandenberghe, W., Nuttin, B., Witjas, T., Régis, J., Azulay, J.P., Eusebio, A., Brown, P., 2018. Beta burst coupling across the motor circuit in Parkinson's disease. Neurobiol. Dis. 117. doi:10.1016/j.nbd.2018.06.007.

Uutela, K., Taulu, S., Hämäläinen, M., 2001. Detecting and correcting for head movements in neuromagnetic measurements. Neuroimage 14. doi:10.1006/nimg.2001.0915.

Vallat, R., 2018. Pingouin–Statistics in python. J. Open Source Softw. 3. doi:10.21105/joss.01026.

Van Ede, F., De Lange, F., Jensen, O., Maris, E., 2011. Orienting attention to an upcoming tactile event involves a spatially and temporally specific modulation of sensorimotor alpha- and beta-band oscillations. J. Neurosci. 31, 2016–2024. doi:10.1523/JNEUROSCI.5630-10.2011.

Velisar, A., Syrkin-Nikolau, J., Blumenfeld, Z., Trager, M.H., Afzal, M.F., Prabhakar, V., Bronte-Stewart, H., 2019. Dual threshold neural closed loop deep brain stimulation in Parkinson disease patients. Brain Stimul. 12. doi:10.1016/j.brs.2019.02.020.

Vinding, M.C., Tsitsi, P., Waldthaler, J., Oostenveld, R., Ingvar, M., Svenningsson, P., Lundqvist, D., 2020. Reduction of spontaneous cortical beta bursts in Parkinson's disease is linked to symptom severity. Brain Commun. 2. doi:10.1093/braincomms/fcaa052.

Whitmer, D., de Solages, C., Hill, B., Yu, H., Henderson, J.M., Bronte-Stewart, H., 2012. High frequency deep brain stimulation attenuates subthalamic and cortical rhythms in Parkinson's disease. Front. Hum. Neurosci. doi:10.3389/fnhum.2012.00155.

Yu, Y., Sanabria, D.E., Wang, J., Hendrix, C.M., Zhang, J., Nebeck, S.D., Amundson, A.M., Busby, Z.B., Bauer, D.L., Johnson, M.D., Johnson, L.A., Vitek, J.L., 2021. Parkinsonism alters beta burst dynamics across the basal ganglia-motor cortical network. J. Neurosci. 41. doi:10.1523/JNEUROSCI.1591-20.2021.